

NEUTRON SPECTRA AND DOSIMETRIC QUANTITIES AT TRANSPORT CASKS FOR REACTOR SPENT FUEL AND VITRIFIED WASTE

A. Rimpler

Federal Office For Radiation Protection, P.O. Box 100149, D-38261 Salzgitter

SUMMARY

Several types of dual purpose casks are used for transport and interim storage of spent fuel assemblies (SFA) and vitrified high-active waste (HAW). Some of these CASTOR-type casks have been stored in the German interim storage facility at Gorleben in recent years.

Generally, radiation exposure of personnel during transportation and storage of spent fuel casks is dominated by neutrons. The forthcoming implementation of the new radiation weighting factor for protection quantities, as well as the new quality factor for the operational quantities as a result of the ICRP 60 recommendation and European Directive in national regulations, will in particular affect the radiological protection during transportation and storage of spent fuel. Therefore, comprehensive measurements of neutron spectra and dose rates were performed at four different cask types, two loaded with spent fuel and two with high-active vitrified waste.

Neutron fluence spectra and dose rates were measured by means of a *Bonner* multisphere spectrometer. The paper briefly describes the experimental method and evaluation procedure. Measured spectra for various locations, types of casks, and inventory are discussed, and compared to calculations with commonly used radiation transport codes.

By folding the spectral distributions with the corresponding conversion coefficients, area doses and effective doses for the old and new quantities were determined and their ratios are given. The neutron area doses around spent fuel casks will increase by approximately 50 % and the effective doses by more than 100 % with the new conventions. This may have practical consequences, if design values of transport casks and transport limits remain unchanged. On the other hand, the former conservatism between measured doses and the primary limiting effective doses decreases significantly.

INTRODUCTION

Several types of containers are used - most of them of the CASTOR-type - for transport and interim storage of spent fuel assemblies from nuclear power plants and vitrified high-active waste from reprocessing. In principle, radiation exposure near these containers is predominated by neutrons. The level and the ratio of gamma and neutron dose rates depend on the fuel history, mainly on the burnup (i.e. total energy produced per unit mass of heavy metal: $\text{GWd}/t_{\text{uranium}}$) and the decay time.

The neutrons originate from spontaneous fission processes, mainly of ^{244}Cm and ^{242}Cm bred from ^{238}U in the fuel during reactor operation, and from (α, n) -reactions at elements with low atomic number. At spent fuel with a burnup of $\geq 30 \text{ GWd}/t_{\text{uranium}}$ about 95 % of the neutrons

are induced by spontaneous fission of ^{244}Cm after a cooling down period of more than two years (Moeller and Burmester 1987). The emission rate due to (α, n) -reactions is negligible for fuel with high burnup which is common for power reactors.

In the case of vitrified waste the neutron output from (α, n) -processes amounts to about 50 % of the total. This is caused by an addition of 10 to 15% boron to the vitrified waste. Boron improves both the mechanical stability of the glass and the criticality safety. The latter is due to the high capture cross section of the isotope ^{10}B for thermal neutrons. On the other hand, boron has a higher efficiency for neutron production by (α, n) -reactions than the oxygen in the UO_2 -fuel. The mean energy is 2.1 MeV for neutrons from spontaneous fission and about 4.5 MeV for (α, n) -processes, respectively.

It was one aim of the work to find out, whether these features of the inventory may result in different neutron spectra outside the casks. Another intention was to investigate, whether the spectral neutron distribution at positions relevant to radiation protection varies for individual cask types and to compare measured spectra with calculated ones. Hence, several series of spectrometric measurements were performed at two containers loaded with spent fuel (CASTOR IIa, CASTOR V19) and at two containers filled with vitrified HAW (CASTOR HAW 20/28, TS 28V). Besides, the measured neutron fluence spectra were used to determine reference values for dose rates aiming at estimating systematic uncertainties of dose rates measured by means of conventional survey meters. The results of these investigations are published in a separate paper at this conference (Boerst et al. 1998).

Moreover, primary attention was given to the expected changes of the numerical data for operational and protection dose quantities, as a result of the implementation of the ICRP 60 recommendations (ICRP 1991). The 'ambient dose equivalent', $H^*(10)$, replaces the formerly used 'maximum dose equivalent', H_{made} , from ICRP 21 (ICRP 1973) in area dosimetry and the 'effective dose', E , substitutes the 'effective dose equivalent', H_E , from ICRP 26 (ICRP 1977) as primary limited body dose. Figure 1 shows the fluence-to-dose conversion coefficients for these quantities in comparison with a typical neutron spectrum at a CASTOR-type container. It is obvious that the 'old' and 'new' quantities differ significantly, even in that energy range where the neutron fluence reaches its maximum.

SPECTROMETRIC METHOD

Neutron fluence spectra at the casks were measured with the *Bonner* multisphere technique (Bramblet et al. 1960). The spectrometric system applied for this work consists of a spherical ^3He proportional counter that is inserted in a set of 5 polyethylene spheres with diameters of 3, 5, 8, 10 and 12 inches (7.6 to 30.5 cm). The fluence response $R_n(E)$ of similar detector/moderator combinations and the bare ^3He counter has been investigated properly (Alevra et al. 1995) and the spectrometer has been adjusted using ISO standard fields at the Physikalisch-Technische Bundesanstalt (PTB). A portable multi-channel analyser was utilised to measure the count rates z_n that result from the integral equation:

$$z_n = \int_E \varphi_E(E) \cdot R_n(E) \cdot dE$$

The deconvolution of the $n = 6$ count rates into the desired spectral fluence rate $\varphi_E(E)$ is performed by an unfolding program using the iterative algorithm of the SAND II code (McElroy et al. 1967). The relatively coarse energy binning of 15 groups between 0.01 eV and

20 MeV seems to be sufficient for calculating integral data such as dose rates with reasonable accuracy for radiation protection purposes. More problems arise, since the number of measurement results (count rates) is smaller than that of the energy bins wanted ('few-channel unfolding'). This can be solved by properly selecting a 'guess-spectrum' that is iteratively modified until the recalculated count rates are statistically compatible with the measured ones. Therefore, the unfolding result is not a unique but a likely solution for the real spectrum. For evaluating the measurements presented in this paper a spectrum calculated with the ANISN radiation transport code was used as start-spectrum (TÜV 1997).

The neutron dose rates \dot{H} were calculated by numerical integration of the unfolded spectrum with the respective fluence-to-dose conversion coefficients $h_{\phi}(E)$ for the dose quantity wanted according to:

$$\dot{H} = \int_E \varphi_E(E) \cdot h_{\phi}(E) \cdot dE$$

The conversion coefficients for the 'maximum dose equivalent' H_{made} were taken from ICRP 21 (ICRP 1973), for the 'effective dose equivalent' H_E from ICRP 26 (ICRP 1977) and those for the 'ambient dose equivalent' $H^*(10)$ and the 'effective dose' E from ICRP 74 (ICRP 1996)¹. The uncertainty of absolute values for doses derived in this way from *Bonner* sphere spectra is assessed to $\pm 20\%$ at maximum.

RESULTS

Appropriate radiation transport codes are available for the shielding design of transport and storage casks as well as for calculating spectra and dose rates at casks with an actual inventory. Among these the MCNP 4A code is one of the most well known. In Fig. 2 a spectrum at the surface of a CASTOR V/19, calculated with this code (TÜV 1997), is compared to a measured one. Both spectra indicate that the primary fission spectrum of the fuel is modified by the 40 cm thick iron walls of the cask, yielding fluence maxima around 100 keV. It is obvious that the calculated spectral distribution has a much better energy resolution, which even shows distinct iron resonances (e.g. at 24 keV). The *Bonner* sphere measurements cannot resolve such details, because of the relatively flat energy dependence of the detector response functions. However, the shape of the spectrum satisfactorily agrees with the calculation. The apparent discrepancies in the thermal energy range are caused by backscatter from the concrete floor during the measurements.

Another question raised was if the type of inventory, i.e. HAW or SFA, influences the spectral distribution outside the casks. Fig. 3a compares spectra at a CASTOR HAW 20/28, loaded with 28 canisters of vitrified waste, and at a CASTOR V/19 with 19 SFA. (In the linear-logarithmic representation equal areas below the histogram correspond to equal numbers of neutrons.) They were measured close to the surface of the side walls at 3 m height from the cask bottom, i.e. at the position where the SFA have the highest burnup. The spectra do not differ distinctively, since the shielding construction of both casks is similar. The different portions and energies of primary neutrons from spontaneous fission and (α , n)-reactions disappear behind the thick iron walls or, at least, they can not be discovered by means of *Bonner* sphere spectrometry.

¹ Note: The symbol E recommended by ICRP 60 for the 'effective dose' is confusing and should not be mixed up with that for the energy E

It is quite another situation when comparing spectra at the lid of both casks. There the spectra obviously disagree, in spite of similar construction and thickness of the lids (see Fig. 3b). Whereas HAW yields a nearly uniform dispersion of the neutron source term, the SFA have a distinctive burnup distribution and a low emission in the top and bottom regions. This fact together with the self-absorption by the fuel assembly top fittings results in a larger effective iron shield at the top of the CASTOR V/19.

Similar effects are visible at casks with different wall construction. The CASTOR HAW 20/28 has an iron wall with 40 cm effective thickness and additional inherent neutron moderator rods of 8 cm diameter each. The wall of the TS 28V, for HAW canisters as well, consists of 28 cm iron with outer neutron shielding segments, 13.5 or 21 cm thick and made of a special resin. As predicted the spectra at both casks disagree (see Fig. 4). The spectrum at the TS 28V shows a considerably higher portion of intermediate neutrons caused by elastic scattering in the external moderator layers. The low thermal neutron fluence is the result of the boron content in the resin. Moreover, the peak between 0.1 and 1 MeV seems to be shifted slightly to higher energies at the TS 28V. This is probably due to the thinner iron wall, 28 cm instead of 40 cm.

Finally, the measured neutron fluence spectra were evaluated to estimate the effect of changes of protection and operational dose quantities by the ICRP 60 recommendations. The results are summarised in Table 1.

CASTOR-type No. of measuring positions	V/19 3	IIa 7	HAW 20/28 6	TS 28V 4
$H^*(10) / H_{\text{made}}$	1.47	1.49	1.49	1.41
$H^*(10) / E$	A-P	1.4	1.5	1.4
	ROT	2.5	2.6	2.7
E / H_E	A-P	2.2	2.5	2.2
	ROT	2.7	3.0	2.7
H_{made} / H_E	A-P	2.2	2.5	2.2
	ROT	4.8	5.3	4.9

Table 1: Ratios of operational and primary dose quantities (mean values from spectra for several locations) and neutron incidence directions (A-P: frontal, ROT: rotational)

At first sight it is obvious that all ratios do not vary by more than about $\pm 10\%$ at the individual casks. The data for $H^*(10)/H_{\text{made}}$ indicate an increase of the numerical values of neutron area doses and dose rates by approximately a factor of 1.5 resulting from the implementation of the new measuring quantity $H^*(10)$. On the other hand, the effective doses will enhance by more than a factor of 2 due to the new radiation and tissue weighting factors according to ICRP 60. Hence, the ratio of measuring and effective dose quantities will decrease.

It is a basic principle in radiation protection that operational quantities should provide a conservative assessment of protection quantities for all exposure conditions. This means in practice: measured doses should overestimate the effective doses for all realistic directions of radiation incidence on the body. For occupational exposure during transport and storage of spent fuel casks frontal (A-P, anterior-posterior) and rotational (ROT) incidence on the body are the most probable cases. As can be seen from H_{made}/H_E in Tab. 1, there was a 'safety factor' of more than 2 between the measured doses and the effective dose equivalents of persons in the past. The implementation of ICRP 60 related quantities will considerably

decrease this inherent safety to a factor of 1.4. Nevertheless, even in the worst case of frontal neutron incidence the effective dose will further be overestimated by about 40 %.

CONCLUSIONS

Neutrons are an important component of radiation exposure during transport and storage of spent fuel assemblies and vitrified waste. The *Bonner* sphere spectrometer has been proven to be a useful tool for detailed analysis of neutron fluence spectra at spent fuel casks and for determining more accurate integral data, such as dose quantities. With some examples of measured spectra for various cask types the influence of several constructive and loading properties on the shape of spectra at locations close to these casks was illustrated. As expected, at very similarly constructed CASTOR-type containers nearly identical spectra were found at comparable locations, independent of the type of inventory.

A major topic of the investigations was to quantify the changes of numerical values of area and body doses as a result of implementing the dose quantities by ICRP 60 in radiation protection practice. Area dose rates will increase by about 50 %. This may have practical and administrative consequences mainly for transportation, if the limits according to the IAEA Safety Standard (IAEA 1985) remain unchanged. The enlargement of effective doses by more than 100 % is of less practical importance in routine dosimetry. However, it has to be considered in cases of unexpected or accidental exposure of persons and if the individual dose limits for occupationally exposed persons are exceeded.

REFERENCES

- Alevra et al. Measurements with the PTB Bonner Sphere Spectrometer and Various Dosimeters Around a Model Storage Cask Filled with a ^{252}Cf Source both free in Air and in a Salt Mine. Report PTB-7.22-95-1, Braunschweig, 1995.
- Boerst et al. Dose Rate Measurements at Several Casks for Transport and Interim Storage. this conference.
- Burmester and Moeller. Calculation of Passive Neutron Emission from Spent WWER-440 fuel. Report SAAS-347, Berlin, 1987.
- IAEA 1985. Regulations for the Safe Transport of Radioactive Material. 1985 Edition (As Amended 1990). Safety Series No. 6, IAEA, Vienna, 1990.
- ICRP 1973. Data for Protection against Ionizing Radiation from External Sources. Publication 21, Oxford: Pergamon Press, 1973.
- ICRP 1977. Recommendations of the International Commission on Radiological Protection. Publication 26, Oxford: Pergamon Press, 1977.
- ICRP 1990. 1990 Recommendations of the International Commission on Radiological Protection. Publication 60, Oxford: Pergamon Press, 1990.
- ICRP 1996. Conversion Coefficients for Use in Radiological Protection against External Radiation. Publication 74, Oxford: Pergamon Press, 1996.
- McElroy et al. A Computer-Automated Iterative Method for Neutron Flux Spectra Determination by Foil Activation. Report AFWL-TR-67-41, Los Alamos, 1967.
- TÜV 1997. Technischer Überwachungs Verein Hannover/Sachsen-Anhalt. Personal communication, 1997.

Fig. 1: Fluence-to-dose equivalent conversion coefficients and CASTOR spectrum

Data for E und H_E for A-P radiation incidence

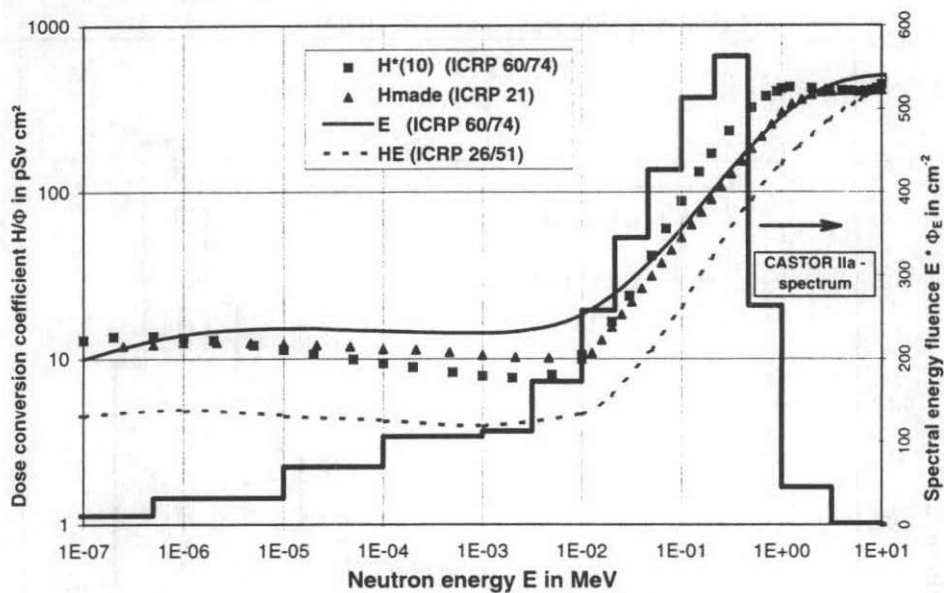


Fig. 2: Neutron spectrum at CASTOR V/19

Comparison measurement / calculation

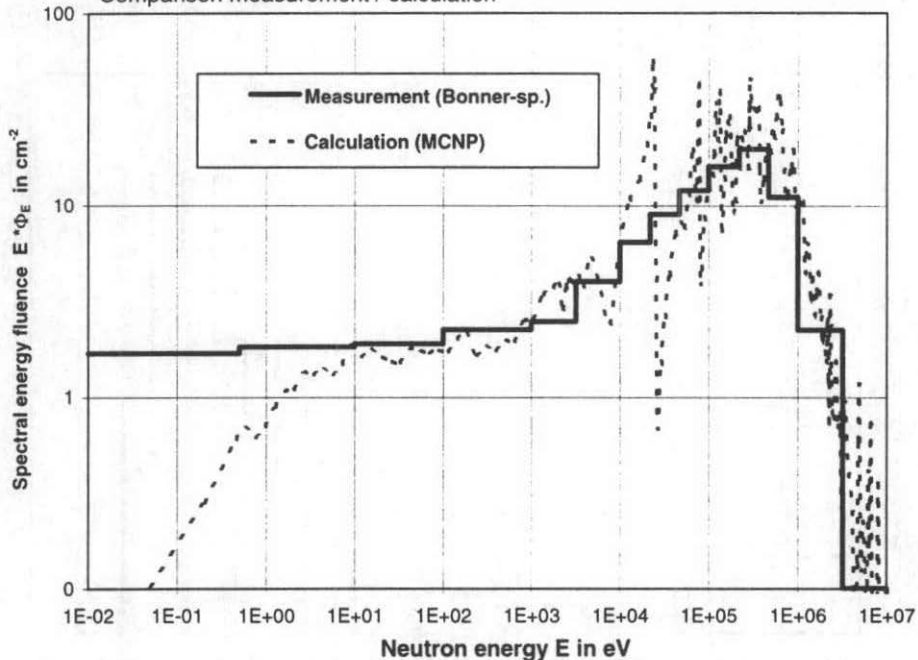


Fig. 3: Neutron spectra at CASTOR V/19 and HAW 20/28
(normalised to fluence maximum)

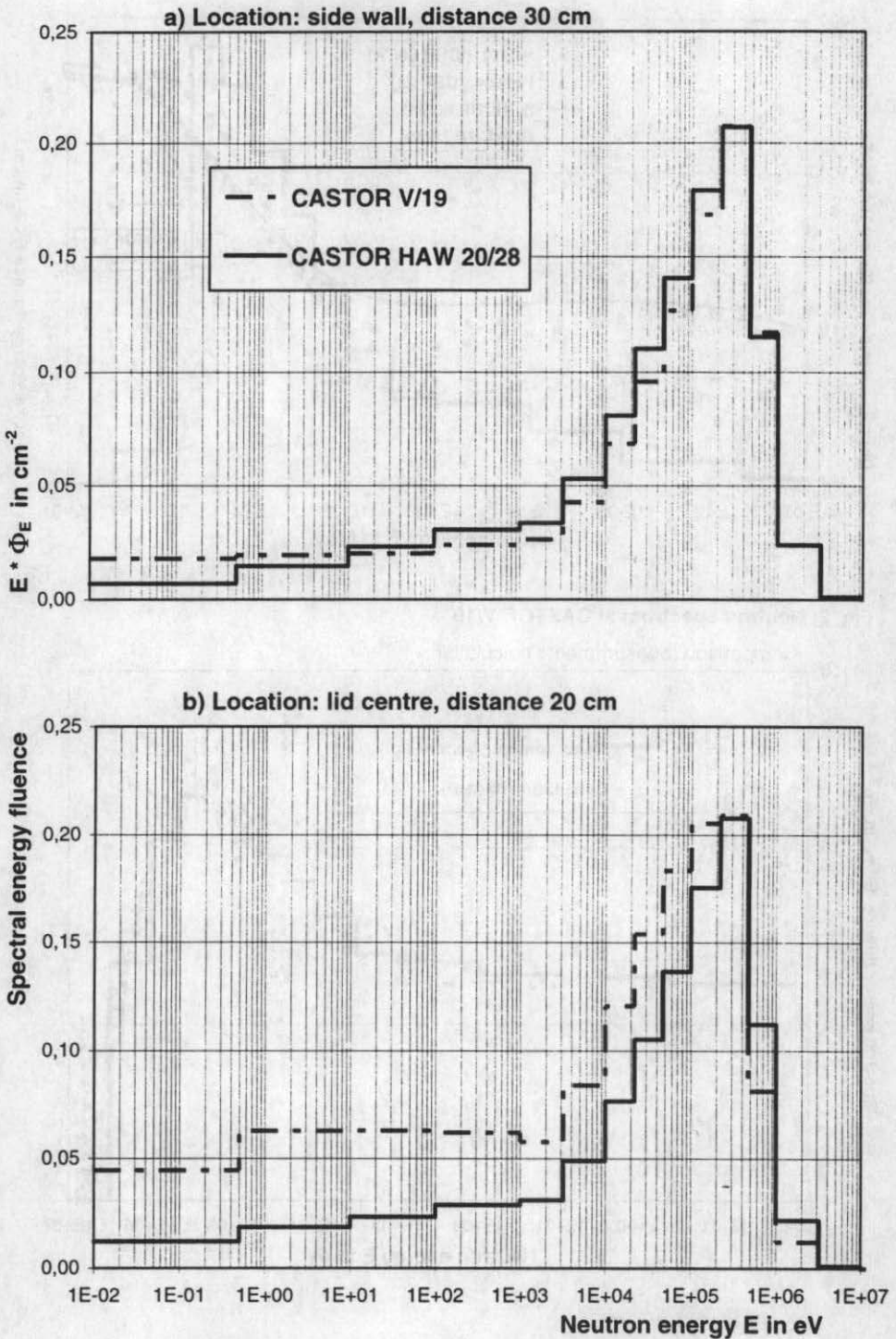
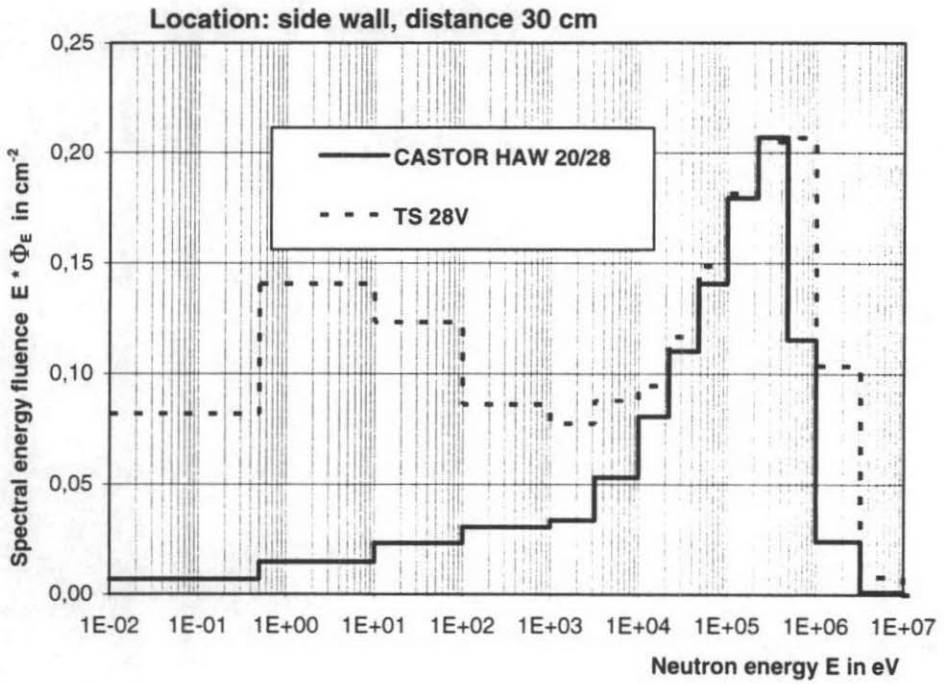
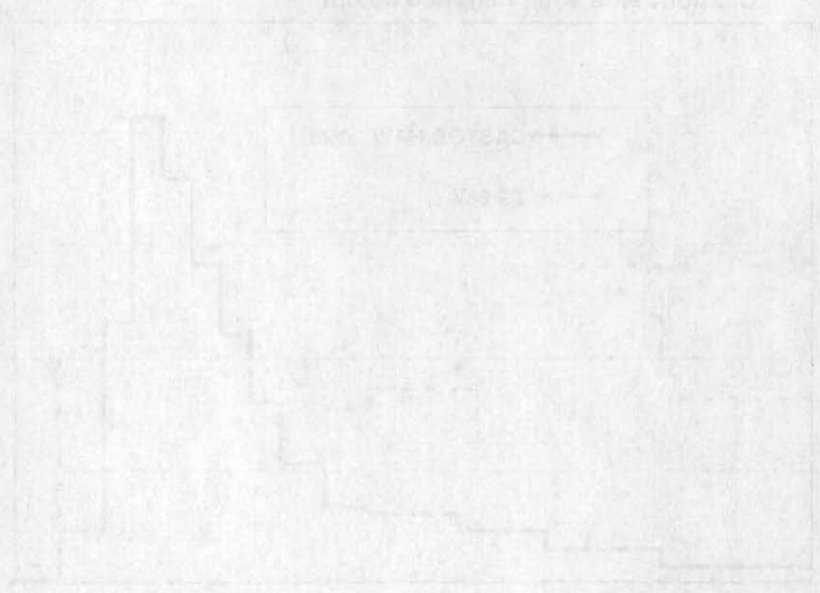


Fig. 4: Neutron spectra at CASTOR HAW 20/28 and TS 28V
(normalised to fluence maximum)





Faint text below the graph, likely a title or description, which is illegible due to the low contrast of the scan.

SESSION 13.2

Regulations

SESSION 1872

REGISTRATION